



**HAL**  
open science

## Mechanisms of innate events during skin reaction following intradermal injection of seasonal influenza vaccine

Jessica Gonnet, Lauranne Poncelet, Celine Meriaux, Elena Gonçalves, Lina Weiss, Nicolas Tchitchek, Eric Pedruzzi, Angele Soria, David Boccara, Annika Vogt, et al.

► **To cite this version:**

Jessica Gonnet, Lauranne Poncelet, Celine Meriaux, Elena Gonçalves, Lina Weiss, et al.. Mechanisms of innate events during skin reaction following intradermal injection of seasonal influenza vaccine. *Journal of Proteomics*, 2020, 216, pp.103670. 10.1016/j.jprot.2020.103670 . hal-03984601v2

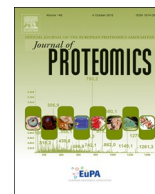
**HAL Id: hal-03984601**

**<https://hal.science/hal-03984601v2>**

Submitted on 20 Mar 2023

**HAL** is a multi-disciplinary open access archive for the deposit and dissemination of scientific research documents, whether they are published or not. The documents may come from teaching and research institutions in France or abroad, or from public or private research centers.

L'archive ouverte pluridisciplinaire **HAL**, est destinée au dépôt et à la diffusion de documents scientifiques de niveau recherche, publiés ou non, émanant des établissements d'enseignement et de recherche français ou étrangers, des laboratoires publics ou privés.



## Mechanisms of innate events during skin reaction following intradermal injection of seasonal influenza vaccine



Jessica Gonnet<sup>a,1</sup>, Lauranne Poncelet<sup>b,c,1</sup>, Celine Meriaux<sup>d,1</sup>, Elena Gonçalves<sup>a</sup>, Lina Weiss<sup>a,e</sup>, Nicolas Tchitchek<sup>f</sup>, Eric Pedruzzi<sup>a</sup>, Angele Soria<sup>a,g</sup>, David Boccara<sup>a,h</sup>, Annika Vogt<sup>a,e</sup>, Olivia Bonduelle<sup>a</sup>, Gregory Hamm<sup>c</sup>, Rima Ait-Belkacem<sup>c</sup>, Jonathan Stauber<sup>c</sup>, Isabelle Fournier<sup>d</sup>, Maxence Wisztorski<sup>d,2</sup>, Behazine Combadiere<sup>a,\*,2</sup>

<sup>a</sup> Sorbonne Université, Centre d'Immunologie et des Maladies Infectieuses – Paris (Cimi-Paris), INSERM U1135, Paris, France

<sup>b</sup> Univ. Lille, INSERM, CHU Lille, U1008 – Controlled Drug Delivery Systems and Biomaterials, F-59000 Lille, France

<sup>c</sup> Imabiotech, 152 rue du Docteur Yersin, 59120 Loos, France

<sup>d</sup> Univ. Lille, Inserm, U1192 – Protéomique, Réponse Inflammatoire et Spectrométrie de Masse-PRISM, F-59000 Lille, France

<sup>e</sup> Clinical Research Center for Hair and Skin Science, Department of Dermatology and Allergy, Charité – Universitätsmedizin Berlin (2), 10117 Berlin, Germany

<sup>f</sup> CEA - Université Paris Sud 11 - INSERM U1184, Immunology of Viral Infections and Autoimmune Diseases, Institut de Biologie François Jacob, 92265 Fontenay-aux-Roses, France

<sup>g</sup> Service de Dermatologie et d'Allergologie, Hôpital Tenon, 4 rue de la Chine, Hôpitaux Universitaire Est Parisien (HUEP), Assistance Publique Hôpitaux de Paris (APHP), 75020 Paris, France

<sup>h</sup> Service de chirurgie plastique reconstructrice, esthétique, centre des brûlés, Hôpital Saint-Louis, Assistance Publique Hôpitaux de Paris (APHP), 1 avenue Claude Vellefaux, 75010 Paris, France

### ARTICLE INFO

#### Keywords:

Skin  
Biomarkers  
Mass spectrometry  
Intradermal vaccination  
Innate immunity

### ABSTRACT

The skin plays a crucial role in host defences against microbial attack and the innate cells must provide the immune system with sufficient information to organize these defences. This unique feature makes the skin a promising site for vaccine administration. Although cellular innate immune events during vaccination have been widely studied, initial events remain poorly understood. Our aim is to determine molecular biomarkers of skin innate reaction after intradermal (i.d.) immunization. Using an ex vivo human explant model from healthy donors, we investigated by NanoLC-MS/MS analysis and MALDI-MSI imaging, to detect innate molecular events (lipids, metabolites, proteins) few hours after i.d. administration of seasonal trivalent influenza vaccine (TIV). This multimodal approach allowed to identify early molecules differentially expressed in dermal and epidermal layers at 4 and 18 h after TIV immunization compared with control PBS. In the dermis, the most relevant network of proteins upregulated were related to cell-to-cell signalling and cell trafficking. The molecular signatures detected were associated with chemokines such as CXCL8, a chemoattractant of neutrophils. In the epidermis, the most relevant networks were associated with activation of antigen-presenting cells and related to CXCL10. Our study proposes a novel step-forward approach to identify biomarkers of skin innate reaction.

**Significance:** To our knowledge, there is no study analyzing innate molecular reaction to vaccines at the site of skin immunization. What is known on skin reaction is based on macroscopic (erythema, redness...), microscopic (epidermal and dermal tissues) and cellular events (inflammatory cell infiltrate). Therefore, we propose a multimodal approach to analyze molecular events at the site of vaccine injection on skin tissue. We identified early molecular networks involved biological functions such cell migration, cell-to-cell interaction and antigen presentation, validated by chemokine expression, in the epidermis and dermis, then could be used as early indicator of success in immunization.

**Abbreviations:** APC, antigen-presenting cells; Dermal DCs, Dendritic cells; FTICR, Fourier-transform ion cyclotron resonance; i.d., Intradermal; IPA, Ingenuity pathway analysis; KCs, Keratinocytes; LCs, Langerhans cells; LFQ, Label-free quantification; MALDI, Matrix assisted laser desorption ionization; MS, Mass spectrometry; MSI, Mass spectrometry imaging; PCA, Principal component analysis; TIV, Trivalent influenza vaccine

\* Corresponding author at: Centre d'Immunologie et des Maladies Infectieuses CIMI-Paris, 91 Boulevard de l'Hôpital, 75013 Paris, France.

E-mail address: [behazine.combadiere@inserm.fr](mailto:behazine.combadiere@inserm.fr) (B. Combadiere).

<sup>1</sup> JG, LP, CM contributed equally to this work

<sup>2</sup> MW and BC contributed equally to this work

<https://doi.org/10.1016/j.jprot.2020.103670>

Received 9 August 2019; Received in revised form 3 December 2019; Accepted 25 January 2020

Available online 25 January 2020

1874-3919/ © 2020 The Authors. Published by Elsevier B.V. This is an open access article under the CC BY-NC-ND license

(<http://creativecommons.org/licenses/by-nc-nd/4.0/>).

## 1. Introduction

The skin's outer surface acts like a suit, forming a physicochemical shield with specialized cells that scan and detect external molecules and danger signals. During barrier disruption (e.g., injuries, vaccination, drug injection), external stimuli reach the epidermal and dermal layer cells. Epidermal cells play a fundamental role in cutaneous innate immunity, providing both a physical barrier via tight junction formation of CD45<sup>neg</sup> keratinocytes (KCs), which constitute up to 90% of the epidermal cell population, alongside the scarcer Langerhans cells (LCs) (1–5% of epidermal cells) [1,2]. Other populations of antigen-presenting cells (APCs), such as dermal dendritic cells (dermal DCs), reside beneath the epidermal layer. Skin epithelial and resident APC subsets take part in antigen uptake and presentation to promote adaptive immunity in human and mouse models [2,3]. Skin barrier disruption provokes the local production of proinflammatory cytokines and chemokines by local skin cells including KCs, LCs, and dermal DCs. How these local resident cells are activated after barrier disruption, starting with the recruitment of inflammatory cells, determines the immunological outcome. However, the early in situ molecular biomarkers of skin reaction to this intrusion remain to be studied.

Our recent work has demonstrated that KCs respond to innate sensors and release IL-32, which allows LCs to detach from the epidermal layer, migrate to the dermis [4], and secrete proinflammatory chemokines and cytokines. These mediators promote inflammatory cell recruitment and APC activation [5–8]. This tissue reaction could reflect inflammatory processes necessary to bridge innate to adaptive immunity. In murine models, intradermal (i.d.) vaccination induces the attraction of neutrophils and monocytes to the immunization site [9,10]. However, initial molecular reaction at the site of immunization needs to be studied. In homeostatic and inflammatory skin tissues [2], several molecules such as mTORC1, the NLRP3 inflammasome, NF- $\kappa$ B signalling, and the MAPK/ERK pathway including EIF4/EIF2 factor transcription have been shown to regulate KCs proliferation and differentiation [11], maturation of skin APCs [12]. Here, we propose to use differential proteomic, lipidomic and metabolomic analysis using NanoLC-mass spectrometry/mass spectrometry (MS/MS) analysis and matrix assisted laser desorption ionization imaging (MALDI)-mass spectrometry imaging (-MSI) to dissect the early molecular events following dermal immunization in a human skin explant model. Seasonal trivalent influenza vaccine (TIV) by i.d. route induces a potent local skin reaction and has been shown to be efficient in the induction of both humoral and T cell responses [13–16]. We thus planned to use TIV injection as a model antigen. We used an ex vivo human skin explant model, which has the advantage of conserving whole tissue architecture. The originality of this work is based on its spatio-temporal proteomic analysis of the epidermis and dermis at different time points after the inoculation. To our knowledge, this study is the first to use an ex vivo human skin explant model for a multiparametric analysis of proteins, lipids, metabolites, and mRNA to explore early cutaneous innate immune events before an inflammatory reaction to a vaccine at the inoculation site.

## 2. Material and methods

### 2.1. Human skin explants

Human skin samples were obtained from healthy volunteers (women aged 21–63 years) undergoing plastic surgery for breast, abdomen, or face lifts (Service de chirurgie plastique, reconstructrice et esthétique - Centre de traitement des brûlés, Saint-Louis Hospital, Paris, France). All skin samples were taken after informed consent in accordance with the local Institutional Ethics Committee guidelines (IRB 00003835) and the ethics rules stated in the Declaration of Helsinki. Skin samples were conserved in NaCl immediately after surgical excision and then processed within 4–6 h post-surgery. They were examined

macroscopically for tissue damage. Either PBS or Intanza® [TIV A/Michigan/45/2015 (H1N1)pdm09, A/Hong Kong/4801/2014 (H3N2), B/Brisbane/60/2008–15  $\mu$ g of haemagglutinin (HA)] (Sanofi-Pasteur, Lyon, France) was administered according to the Mantoux method by i.d. injection. In all, 45  $\mu$ g of total HA protein/cm<sup>2</sup> of skin (volume: 25  $\mu$ L of Intanza® and 15  $\mu$ g of HA for each influenza strain) was injected in the dermis. Intanza formulation (100  $\mu$ L) was diluted to a quarter to be injected in each of the 1 cm<sup>2</sup> pieces of skin. Influenza vaccine and PBS control injected skin were incubated 4 and 18 h, draining in RPMI 1640 medium (Gibco® Thermo Fisher Scientific, Waltham, MA, U.S.A.). As Fig. 1 shows, skin donors ( $n = 6$ ) were used both for cryosection for analysis by MALDI-Fourier-transform ion cyclotron resonance (-FTICR) and for epidermal and dermal cell suspensions for high throughput proteomic analysis. Skin samples were also used to validate cytokine and chemokine expression by qPCR (supplemental materials).

### 2.2. Skin epidermal and dermal layers

After the injections into fresh skin samples (1 cm<sup>2</sup>), the tissue was cut into small pieces and incubated in RPMI 1640 medium with 2.4 IU/ml of dispase II (Sigma-Aldrich, St. Louis, MO, U.S.A.) overnight at 4 °C with agitation to separate epidermal sheets from the dermis. Epidermal sheets were then removed from the dermis with mechanical tweezers. Epidermal cell suspensions were obtained after 10 min incubation at 37 °C in RPMI 1640 and trypsin-EDTA 0.2% (Sigma-Aldrich), supplemented with DNase I (10  $\mu$ g/mL, Roche, Boulogne Billancourt, France). Fetal calf serum (FCS, Dominique Dutscher, Brumath, France) was then added. Cell suspensions were washed in RPMI 1640 + 20% FCS medium, processed through a 70- $\mu$ m filter (Falcon BD™, San Jose, CA, U.S.A.), and then washed in PBS. Cell pellets were dried, then frozen and conserved at –80 °C.

### 2.3. Protein detection and identification

See the supplementary information for the detailed protocol. Briefly, dermal and epidermal cells (the equivalent of 2 million cells for each condition) were lysed and proteins extracted with a Radioimmunoprecipitation assay (RIPA) buffer. Extracted proteins were digested with filter-aided sample preparation (FASP), and the peptides retrieved were analysed with a nanoUPLC system coupled with a high-resolution mass spectrometer for MS and MS/MS analysis. The detailed methods are described in the supplemental materials and methods section.

All MS data were processed with MaxQuant (version 1.5.6.5) by using the Andromeda search engine. The proteins were identified by searching MS and MS/MS data against the reviewed proteome for *Homo sapiens* in the UniProt database (Release February 2017, 20,172 entries) and 262 commonly detected contaminants. Trypsin specificity was used for digestion mode. N-terminal acetylation and methionine oxidation were selected as variable modifications and carbamidomethylation of cysteines as fixed. Up to two missed cleavages were allowed. An initial mass accuracy of 6 ppm was selected for MS spectra. The MS/MS tolerance was set to 20 ppm for the HCD data (higher-energy-collisional-dissociation). False discovery rates for peptide spectrum matches and for protein identifications were estimated by using a decoy version of the previously defined databases (reverse construction) and set at 1%. Relative label-free quantification (LFQ) of the proteins was conducted with MaxQuant, by applying the MaxLFQ algorithm with default parameters. Analysis of the identified proteins was performed with Perseus software (<http://www.perseus-framework.org>) (version 1.5.6.0). The file containing the information from the identification was used. Hits from the reverse database and proteins with only modified peptides were removed. Hits from potential contaminants were marked, and proteins originating from culture medium (e.g., serum albumin from *Bos taurus*) or sample preparation (e.g., trypsin from *Sus scrofa*)

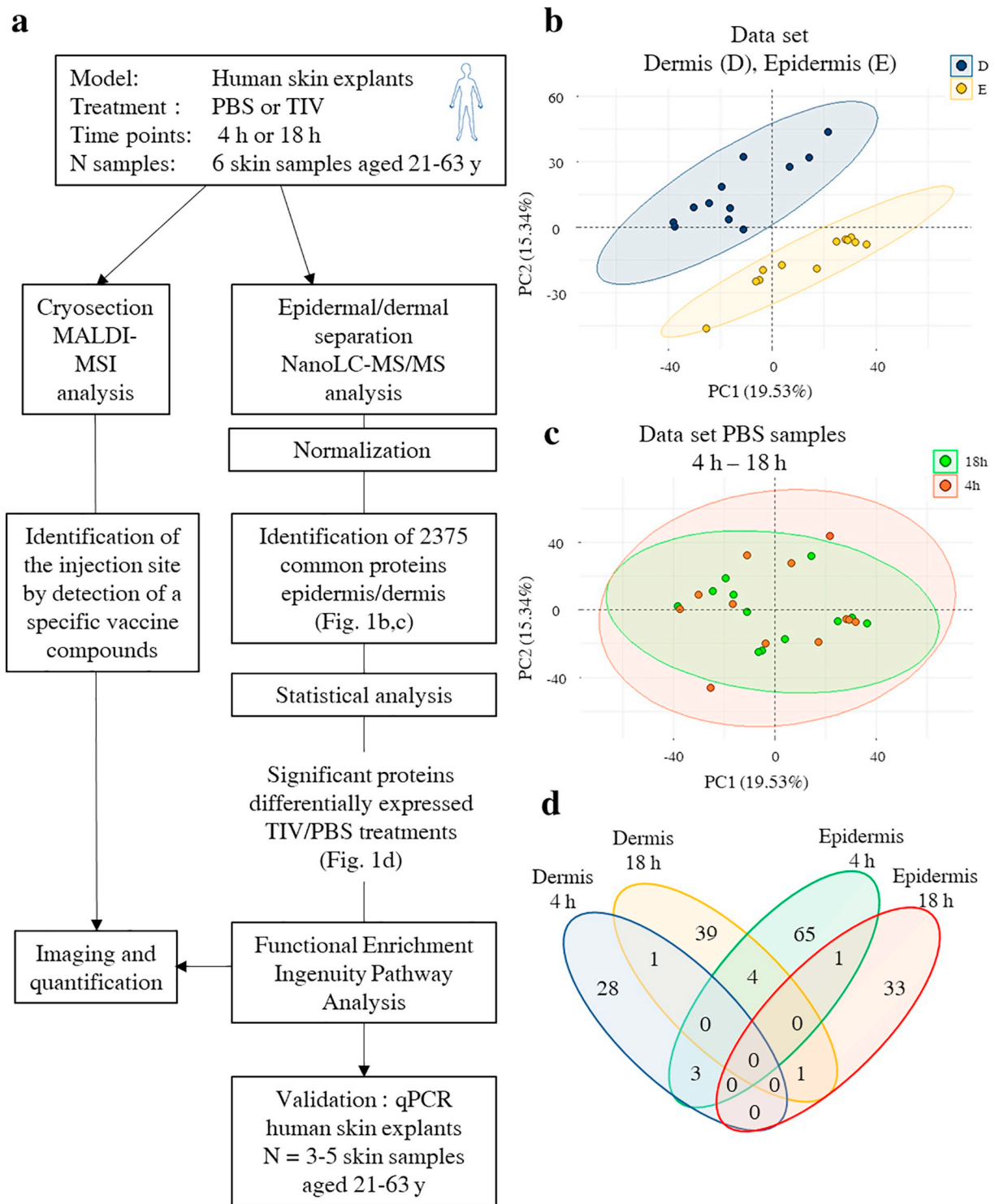
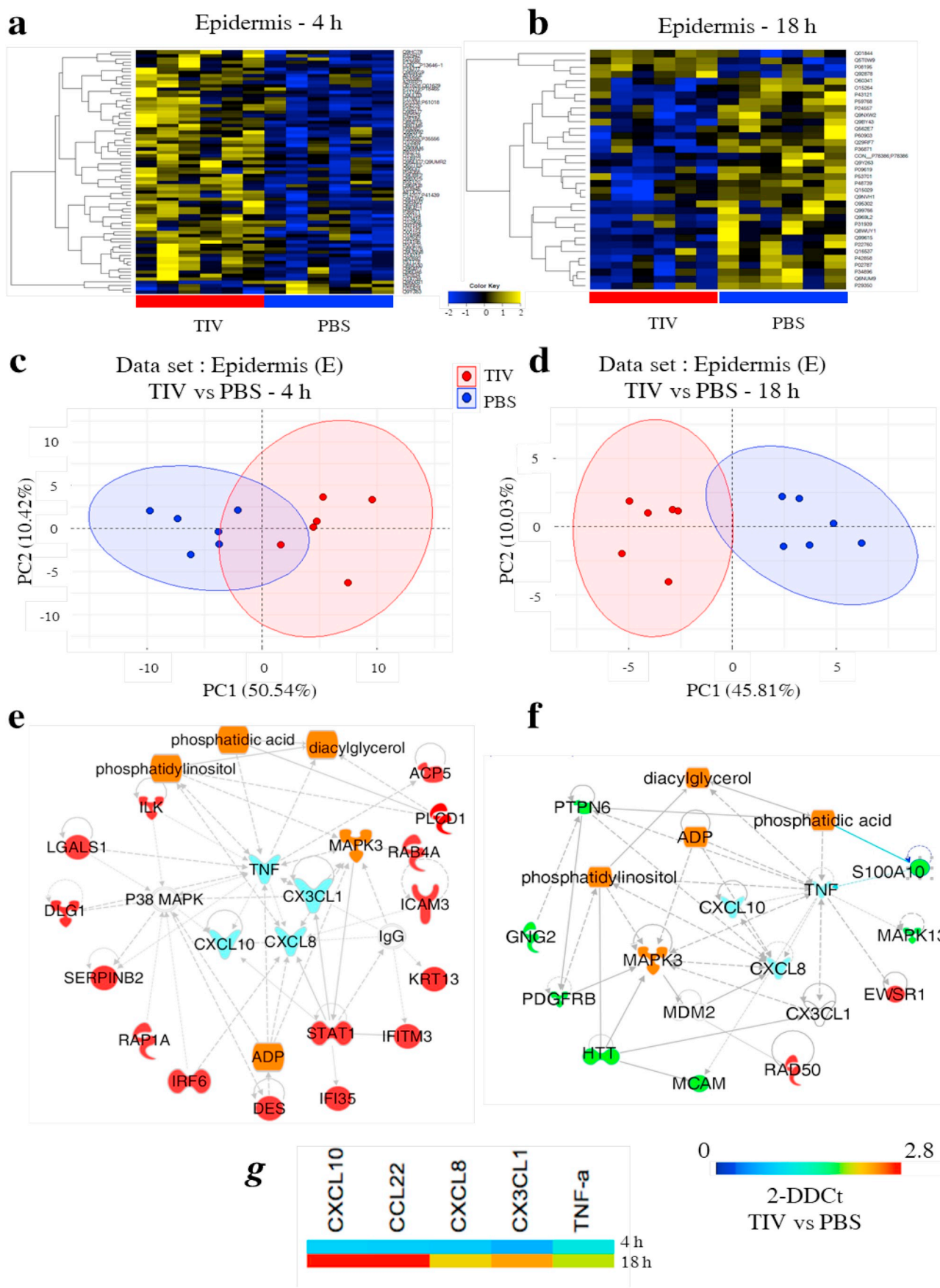


**Fig. 1.** A multimodal approach of early innate events during skin reaction following intradermal injection of seasonal influenza vaccine. (a) **Flow Chart:** Human skin samples from six healthy donors (women aged 21–63 years), were cut into 1-cm<sup>2</sup> pieces after injection by TIV (Intanza®, microneedle device) or PBS by the i.d. route. Samples either underwent enzymatic digestion (flow chart, right) or cryopreservation (flow chart, left) for in situ investigation by MALDI-MSI of modifications in lipids and metabolites. Epidermal and dermal cell suspensions were used for proteomic analyses: the protein lysate was analysed by NanoLC-MS/MS; the peptide sequence analyses were processed by Maxquant software, and contaminants removed; and common proteins ( $n = 2375$ ) were identified in the epidermis and dermis after TIV and PBS administration. Following statistical analysis using Wilcoxon signed rank test,  $P$ -value < .05. Statistical analyses were performed with R software (Wilcoxon matched-pairs signed rank test, with a two-sided  $P$ -value of < 0.05). The Ingenuity Pathway Analysis (IPA) program was applied on significant proteins, to identify top gene networks and biological function. Gene expression was measured on mRNA samples extracted from the same donors ( $n = 3–5$  donors) by RT-qPCR. (b,c) Score plot from the PCA of all PBS samples based on the detection profiles of the 2375 proteins detected. (b) Projections of PC1 (19.53% of the total variance) and of PC2 (15.34%) separate the dermal (blue dots) and epidermal (yellow dots) samples defined by two concentration ellipses, (c) but do not separate 4 h (red dots) from 18 h (green dots) samples. (d) Venn diagram representing number of proteins significantly differentially detected in TIV compared to PBS in epidermis and dermis at 4 h and 18 h. (For interpretation of the references to colour in this figure legend, the reader is referred to the web version of this article.)



(caption on next page)

**Fig. 2.** Identification of early inflammatory proteins and metabolites induced in the epidermis in response to i.d. TIV administration.

(a, b) Data set of significant proteins in the epidermis are represented in a heat-maps with the level of detection in TIV-treated compared to PBS-control skin at 4 h (a) and 18 h (b) (Wilcoxon matched-pairs signed rank test,  $P$ -value < .05). (c,d) Score plots from the PCA are represented based on detection profiles of the 73 and 35 significant proteins differentially expressed between treated (red dots) and control (blue dots) samples at the 4 h condition (c) and 18 h (d) respectively. (e, f) Top networks from IPA highlighting major proteins from comparison of TIV and control conditions at 4 h (e) and 18 h (f). Overexpression after trivalent influenza vaccine (TIV) administration is represented in red, overexpression for the PBS condition in green. In orange the metabolites and lipids and in blue the proinflammatory cytokines found linked to the proteins of interest. In white, the proteins added by IPA, to complete the top network but not identified in our study. Solid lines = direct relations, dashed lines = indirect relations. (g) mRNA expression analysis in epidermal cells injected with either TIV or PBS. Gene expression was normalized to the mean of actin and GAPDH expression and presented as relative fold gene expression levels compared to PBS controls, after calculating the  $2^{-\Delta\Delta Ct}$  values. (For interpretation of the references to colour in this figure legend, the reader is referred to the web version of this article.)

were manually removed to ensure that only proteins that are part of the human skin structure were retained. LFQ intensities were transformed by base 2 logarithm before statistical analysis.

#### 2.4. Statistical analysis

Protein expression data were analysed using R software. Analysis of the difference between TIV and PBS conditions at each time point was based on a paired nonparametric  $t$ -test (Wilcoxon signed-rank test), with a two-tailed test ( $p$ -value < .05) considered a statistically significant. Unsupervised multivariate analysis was performed using Principal Component Analysis (PCA) using R software. Heatmaps and hierarchical clusters were generated with R software based on the Pearson coefficient of correlation with the complete linkage method.

#### 2.5. Data availability statement

The normalized proteomic data that support the findings of this study have been deposited in ArrayExpress with the accession code. The mass spectrometry proteomics data have been deposited to the ProteomeXchange Consortium via the PRIDE [17] partner repository with the dataset identifier PXD017313.

### 3. Results and discussion

#### 3.1. A multimodal approach of early innate events during skin reaction following intradermal injection of seasonal influenza vaccine

Using an ex vivo human skin explant model, we examined the cutaneous early innate molecular events induced at early time points (4 and 18 h) after TIV administration. Of note, skin explants is an ex vivo model that allows the investigation of early tissue reaction without inflammatory cells recruitment (absence of blood flow). We have previously showed that 3–4 h after intradermal injection in the skin explants allows the detection of KC and LC activation to several intradermal stimuli (nanoparticle vaccine, modified vaccinia Ankara and Toll-like receptor ligands) [4,18]. We also showed LC renewal in the epidermis at 18 h post i.d. injection of MVA [18] while inflammatory cells continue to migrate to the dermis [19]. We thus have chosen these time points for the further omics analysis. Fig. 1a presents the experimental plan. Skin explants from 6 healthy donors were injected by i.d. route with either TIV or PBS. For each donor, we divided skin samples in two parts: 1) dermal and epidermal cell suspensions were prepared for protein identification with MS-based proteomics at 4 and 18 h after treatment; 2) skin tissue sections were cryopreserved for in situ analysis by MALDI-MSI of metabolite and lipid alteration (Fig. 1a, flow chart, left branch). Results of LFQ proteomics were analysed to identify the significant proteins (that is, those with significantly differential expression) detected after TIV and PBS administration (Fig. 1a, flow chart, right). Finally, we used the IPA program to explore networks and pathways (Fig. 1a).

First, NanoLC-MS/MS analyses of dermal and epidermal cell suspensions allowed the identification of 2.375 common proteins. Principal Component Analysis (PCA) of all samples, restricted to this list

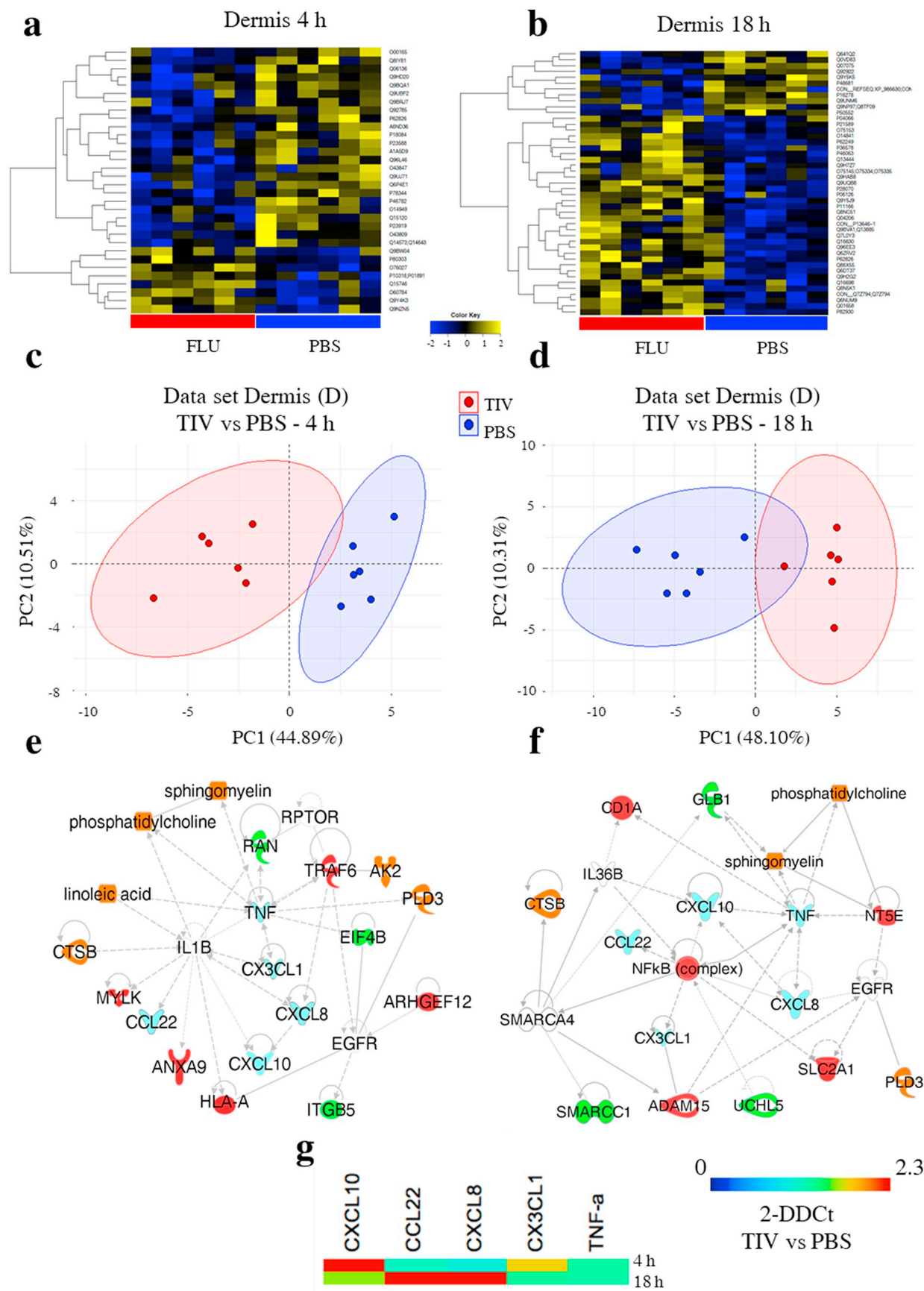
of 2.375 proteins, separated the dermal and epidermal samples (Fig. 1b). Accordingly, the dermal and epidermal samples differed significantly in their protein detection levels and were therefore studied separately. In addition, control skin incubated for 4 or 18 h after PBS injection did not differ in protein detection levels at either time point, as PCA showed (Fig. 1c). Additional analysis of the impact of age on protein distribution showed no difference between those individuals < 35 years and > 35 years (data not shown).

In the epidermis, we found 73 significant proteins detected at 4 h and 35 proteins at 18 h that were differentially expressed after TIV compared with PBS injection (Wilcoxon signed-rank test,  $P$ -value < .05) (Fig. 1d, Supplemental Table 1). In the dermis, we found 32 proteins at 4 h and 45 proteins at 18 h detected with significantly differential expression after TIV injection compared with PBS (Wilcoxon signed rank test,  $P$ -value < .05) (Fig. 1d, Supplemental Table 3). The Venn diagram in Fig. 1d showed significant proteins, exclusive to the treatment condition and tissue layer with only few shared molecules, suggesting specific molecular events in each skin layer.

#### 3.2. Identification of early inflammatory proteins and metabolites induced in the epidermis in response to i.d. TIV administration

Heat-maps represent the detection levels of significant proteins (73 and 35 proteins differentially detected at 4 h and 18 h after treatment, respectively) in the epidermis of TIV-treated compared with PBS control skin at 4 and 18 h (Fig. 2a and b, Supplemental Table 1). The PCA of all samples based on these proteins, separated TIV-treated from PBS control skin at both time points (Fig. 2c, d).

We performed a functional enrichment analysis using Ingenuity Pathway Analysis (IPA), in order to understand the involvement of these proteins in immune functions. Supplemental Table 2 summarizes the top upregulated and downregulated proteins and their contributions to immune responses in the epidermis at, respectively, 4 h and 18 h. The Top IPA biological functions are cell-to-cell signalling and interaction (IPA:  $P$ -value =  $1.53 \times 10^{-3}$  -  $4.75 \times 10^{-2}$ ), cellular assembly and organization (IPA:  $P$ -value =  $3.39 \times 10^{-4}$  -  $4.31 \times 10^{-2}$ ), and immune cell trafficking (IPA:  $P$ -value =  $2.41 \times 10^{-3}$  -  $4.05 \times 10^{-2}$ ). Among major proteins, IFITM3, STAT1, and IFI35 are involved in interferon signalling (IPA:  $P$ -value =  $3.09 \times 10^{-4}$ ), while ICAM3 participates in cross-talk between cells (IPA:  $P$ -value =  $3.2 \times 10^{-4}$ ) and PLCD1 with STAT1 in DC maturation (IPA:  $P$ -value =  $4.75 \times 10^{-3}$ ) (Supplemental Table 2). STAT 1 is involved as well in the TH17 pathway, which is also a proposed outcome of skin immunization [4,18]. At 4 h after i.d. TIV administration, we detected the upregulation of ILK, LGALS1, SERPINB2, and IRF6, which are reported to contribute respectively to cutaneous wound contraction, wound healing, defects of the stratum corneum, and KC differentiation [20–23]. We also found the following proteins to be upregulated: IFI35, an inflammatory marker observed in skin lesions from atopic dermatitis [24], IFITM3, the expression of which increases on T cells after viral infection [25], and IRF6, which, driven by TLR3 activation, plays a role in KC cytokine expression [26]. Also notably upregulated were ICAM3 [27], HLA-B, and HLA-DRB5 [28] — all proteins allowing antigen presentation (IPA:  $P$ -value =  $8.54 \times 10^{-3}$ ).



(caption on next page)

**Fig. 3.** Identification of early inflammatory proteins and metabolites induced in the dermis in response to i.d. TIV administration.

(a, b) Data set of significant proteins in the dermis are represented in a heat-maps with the level of detection in TIV-treated compared to PBS-control skin at 4 h (a) and 18 h (b) (Wilcoxon matched-pairs signed rank test,  $P$ -value < .05). (c,d) Score plots from the PCA are represented based on detection profiles of the 32 and 45 significant proteins differentially expressed between treated (red dots) and control (blue dots) samples at the 4 h condition (c) and 18 h (d) respectively. (e, f) Top networks from IPA highlighting major proteins from comparison of TIV and control conditions at 4 h (e) and 18 h (f). Overexpression after trivalent influenza vaccine (TIV) administration is represented in red, overexpression for the PBS condition in green. In orange the metabolites and lipids and in blue the proinflammatory cytokines found linked to the proteins of interest. In white, the proteins added by IPA, to complete the top network but not identified in our study. Solid lines = direct relations, dashed lines = indirect relations. (g) mRNA expression analysis in epidermal cells injected with either TIV or PBS. Gene expression was normalized to the mean of actin and GAPDH expression and presented as relative fold gene expression levels compared to PBS controls, after calculating the  $2^{\text{ddCt}}$  values ( $n = 3-5$ ). (For interpretation of the references to colour in this figure legend, the reader is referred to the web version of this article.)

Supplemental Table 2 describes the proteins making major contributions to immune responses at 18 h. We found 9/35 proteins in the major IPA biological functions (Fig. 2f). Most of these molecules were downregulated in the skin at 18 h (in green) and are involved in inflammatory responses (IPA:  $P$ -value =  $1.73 \times 10^{-3}$  -  $2.10 \times 10^{-2}$ ), cell-to-cell signalling and interaction (IPA:  $P$ -value =  $1.73 \times 10^{-3}$  -  $1.20 \times 10^{-2}$ ), cell movement (IPA:  $P$ -value =  $1.73 \times 10^{-3}$  -  $1.89 \times 10^{-2}$ ), or macrophage functions (e.g., S100A10, HTT, MAPK13, PTPN6, GNG2, and MCAM) (IPA:  $P$ -value =  $4.46 \times 10^{-3}$  -  $1.13 \times 10^{-2}$ ).

The protein networks significantly detected in the epidermis after TIV injection were connected to proinflammatory cytokines and chemokines, which we measured by qPCR analysis in epidermal cells before and after treatment. Fig. 2g shows the mean gene expression in epidermal cell suspensions for 5 healthy donors. We observed significant increased expression of CX3CL1, CCL22, CXCL10, CXCL8, and TNF $\alpha$  genes at 4 h and 18 h after i.d. TIV injection.

### 3.3. Identification of early inflammatory proteins and metabolites induced in the dermis in response to i.d. TIV administration

Significant detected proteins that are differentially expressed in the dermis for TIV-treated skin compared with PBS controls at 4 h and 18 h are represented in the heat maps (Fig. 3a, b, respectively). In the dermis, we found 32 significant proteins detected differentially at 4 h and 45 proteins at 18 h after TIV compared with PBS injection (Supplemental Table 3). The PCA of all samples was based on the detection profiles of these genes, and the score plots showed that the projections of PC1 (44.89% of the total variance for dermis 4 h and 48.10% for 18 h) and of PC2 (10.51% for epidermis 4 h and 10.31% for 18 h) separated TIV-treated from PBS control skin for the dermal layer at both time points (Fig. 3c, d). We performed a functional enrichment analysis using IPA for identification of top immunological pathways. Supplemental Table 4 summarizes the proteins that were upregulated and downregulated in the dermis in TIV-treated skin compared to PBS controls. These are mostly involved in cell-to-cell signalling and interaction (IPA:  $P$ -value =  $6.29 \times 10^{-3}$  -  $2.19 \times 10^{-2}$ ) and interaction markers associated with skin inflammation (IPA Inflammation Response:  $P$ -value =  $4.72 \times 10^{-3}$  -  $2.34 \times 10^{-2}$ ). TRAF6 is one of them; its involvement in DC maturation (IPA:  $P$ -value =  $3.43 \times 10^{-2}$ ) makes it an interesting biomarker of innate immunity for adaptive responses. Other downregulated molecules include EIF4B, which has been linked to mTOR signalling (IPA:  $P$ -value =  $3.63 \times 10^{-3}$ ) and identified as an essential regulator in skin morphogenesis [29]. Interestingly, MYLK, a protein involved in cell morphology (IPA:  $P$ -value =  $7.86 \times 10^{-3}$  -  $3.41 \times 10^{-2}$ ), was upregulated, and changes in the morphology of LCs but also DCs upon activation or danger signals are among the main features of skin APCs [2,4,12,18]. In the dermis, the production of some inflammatory markers was modified, including the well-known NF $\kappa$ B subunit and TRAF6 [30], as well as markers such as ITGB5 and HLA-A, which have been observed in particular in inflammatory skin disorders and cutaneous adverse reactions [31,32]. We also noted the upregulation of CD1a and the downregulation of CD207, markers that might account for the migration of LCs and CD207+ dermal DCs after their activation, respectively to the dermis and draining lymph nodes during

cell trafficking [3,18]. Finally, PSMB4 and PSMD13, both proteins involved in the proteasome complex, which is crucial for antigen presentation, were also deregulated [33,34].

At 18 h, 11/45 molecules, all upregulated in TIV-treated skin, were involved in multiple mechanisms (Supplemental Table 4), such as cell signalling and interaction (IPA:  $P$ -value =  $2.29 \times 10^{-3}$  -  $4.09 \times 10^{-2}$ ), cell repair (IPA:  $P$ -value =  $2.29 \times 10^{-3}$  -  $4.92 \times 10^{-2}$ ), cell movement (IPA:  $P$ -value =  $4.57 \times 10^{-3}$  -  $4.70 \times 10^{-2}$ ), injury (IPA:  $P$ -value =  $2.29 \times 10^{-3}$  -  $4.72 \times 10^{-2}$ ), metabolism (IPA:  $P$ -value =  $2.29 \times 10^{-3}$  -  $4.92 \times 10^{-2}$ ), molecular transport (IPA:  $P$ -value =  $2.29 \times 10^{-3}$  -  $4.04 \times 10^{-2}$ ), and the cell cycle (IPA:  $P$ -value =  $9.13 \times 10^{-3}$  -  $3.38 \times 10^{-2}$ ). These activities suggest massive reorganization and repair in the dermis — the site of injection of the vaccine compounds.

Because most of these molecules are also associated with inflammatory mediators, we measured the expression of the genes for these proinflammatory cytokines and chemokines, in connection with the protein network significantly detected by qPCR analysis of epidermal cells after TIV injection in the dermis. Fig. 3g shows the mean gene expression in the dermal cell suspension in 5 healthy donors. We observed an increase in gene expression of CXCL10 at the early time points and of CCL22 and CXCL8 at 18 h after i.d. TIV administration.

### 3.4. Identification of major metabolites induced in the skin in response to i.d. TIV administration

As shown in Figs. 2 and 3, IPA pathways highlighted several metabolites and lipids potentially involved in top networks and may indicate changes in epidermal and dermal cellular processes. MALDI-FTICR has proved its efficacy in detection drug compounds and small molecules on skin explant tissue section imaging [35,36]. Using MALDI-FTICR, we performed in situ analyses on skin cryosections treated for 4 h compared with PBS controls (Supplemental Fig. 1). The vaccine injection area was detected in the skin of 6 donors by a vaccine excipient, i.e. Octoxinol 10 (Supplemental Fig. 1, left images). No detection of the vaccine excipient was found on PBS skin tissue section (right images). Based on IPA data base, metabolites and lipids potentially involved in top networks were analysed on tissue sections. As Fig. 4a shows fold-changes of mean intensity of 8 metabolites and lipids (highlighted in IPA analysis), including phosphatidylcholine (PC) (32:0) and (36:1), phosphatidylinositol (PI) (34:1), diacylglycerol (DG) (34:1), adenosine diphosphate (ADP), linoleic acid (LA) (FA 18:2), phosphatidic acid (PA) (18:1), and sphingomyelin (SM) (d34:1), observed in TIV-treated skin compared to PBS controls, for each skin layer (Fig. 4a). PA (18:1) ( $P$ -value = .049) and ADP or dGDP ( $P$ -value = .006) were overexpressed in the TIV condition and localized in the epidermis. Whereas LA ( $P$ -value = .05) was overexpressed in the TIV condition and localized in the dermis. PA (18:1) was overexpressed in the TIV condition and localized in the epidermis. Fig. 4b shows the molecular distribution of PA (18:1) on skin and underlines that it was principally overexpressed in epidermis and at the top of the dermis. The molecular distribution of this lipid was homogenous inside the epidermis tissue. Fig. 4c shows the molecular distribution of LA on each tissue. Mass spectrometry imaging (MSI) enabled the visualization of this compound's overexpression in the dermis and epidermis. It is now



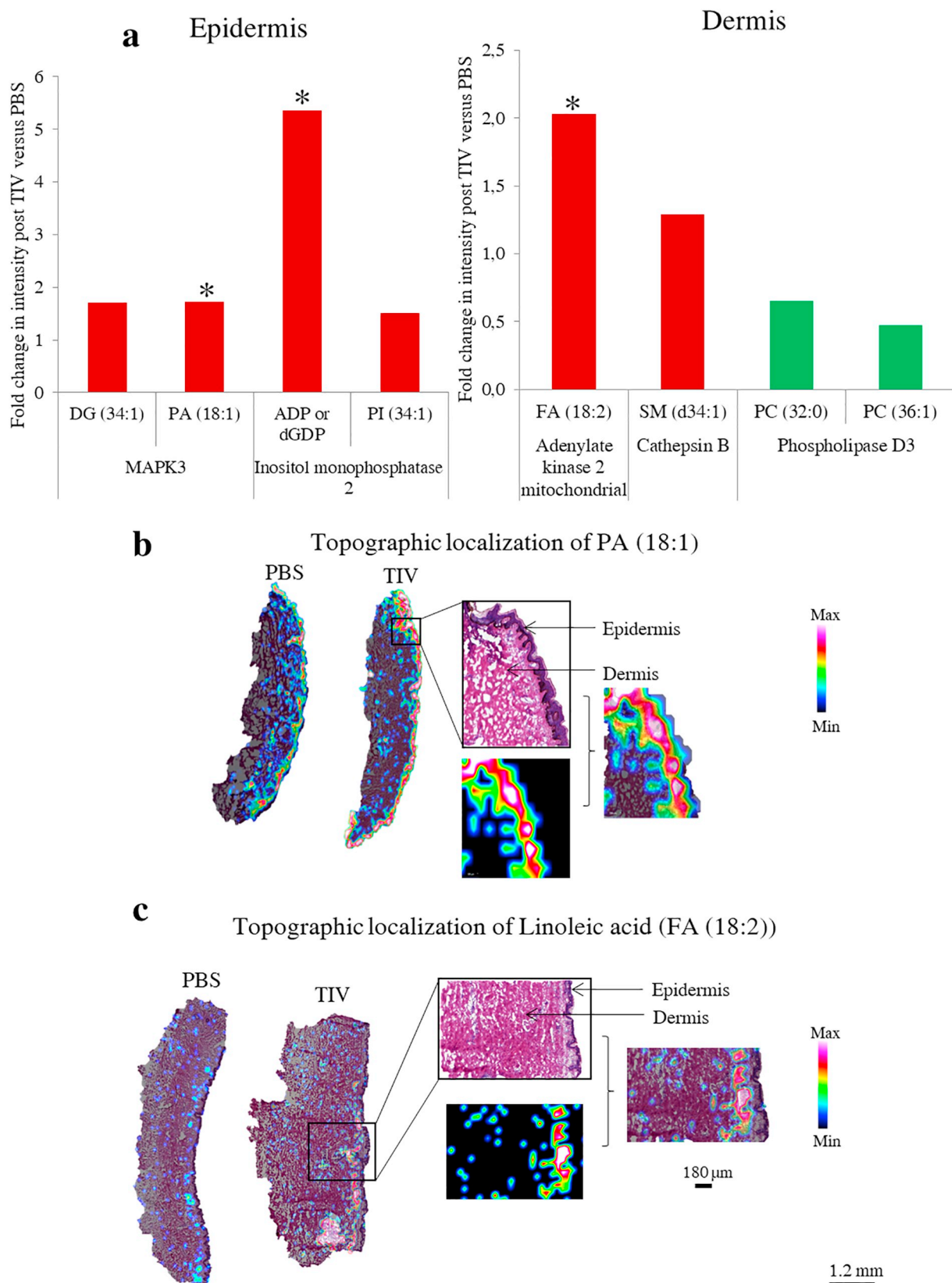


**Fig. 4.** Identification of major metabolites induced in the skin in response to i.d. TIV administration. (a) Metabolites and lipids expression level in the epidermis (left) and in the dermis (right), according to IPA analysis. The fold changes of intensity were calculated comparing the TIV and PBS conditions. Overexpression after trivalent influenza vaccine (TIV) administration is represented in red, overexpression for the PBS condition in green. (b) Representative MALDI-MS imaging of PA (18:1) measured at  $m/z$  435.2517 in TIV and PBS treated skins (c) Representative MALDI-MS imaging of Linoleic acid (FA 18:2) measured at  $m/z$  279 in TIV and PBS treated skin. DG: diacylglycerol; ADP: adenosine 5'-diphosphate; dGDP: 2'-deoxyguanosine 5'-diphosphate; PI: phosphatidylinositol; LA: linoleic acid, FA: fatty acid; SM: sphingomyelin; PC: phosphatidylcholine. (For interpretation of the references to colour in this figure legend, the reader is referred to the web version of this article.)

well established that lipids and metabolites affect cutaneous innate immunity [37,38]. The mass spectrometric analyses showed the in situ modulation of metabolites and lipids related to proteins previously detected, such as MAPK3 and phospholipase D3 involved in immune signalling. Indeed, SM molecules detected in the dermis, are known to be related to such antimicrobial peptides as cathepsin B. Changes in SM and ceramide content have also been reported to affect membrane physiology directly, thus modifying signal transmission and interfering with diverse aspects of T cell activity [39]. For example, long-chain polyunsaturated fatty acids, such as LA (FA (18:2)), have immunoregulatory functions via several mechanisms [40]. Some long-chain polyunsaturated fatty acids are precursors of lipid mediators [41], which participate in inflammatory processes and also affect acquired immune cells.

DG and PA, observed in the epidermis, have demonstrated links to signalling kinase proteins MAPK3. Moreover, DG can act as a second messenger to activate many downstream signalling cascades. DG has been an established ligand for protein kinase C isoforms that can influence inflammation [42,43]. We found additional dermal and epidermal molecules, detected by MALDI-MSI, such as LA, PC, ADP, and inositol phosphate detected in situ, thus demonstrating their effect in cutaneous immunity. Furthermore, PC in the form of several lipids, such as lysophosphatidic acid (LPA) (lysoPA), lysophosphatidylcholine (lysoPC), PI, and PA, has been observed to be expressed differentially in psoriasis patients compared with healthy volunteers [44]. Extracellular nucleotides such as ADP have also demonstrated their role in the regulation of DCs and of other immune cell functions, through their activation of some G-protein coupled receptors called P2 receptors or via ADP ribosylation, which increases the cAMP concentration [45]. Finally, inositol phosphate is reported to modulate the secretion of cytokines derived from both T and myeloid cells (IL-1 $\beta$ , IL-6, and IL-22) and TNF- $\alpha$  [46]. Accordingly, these mediators promote the recruitment of inflammatory cells such as neutrophils but also monocytes, which also play a role in the transport of antigens from the skin to the lymph nodes during inflammation; they also participate in CD8 T cell priming in the bone marrow and inflammatory signals in the lymph nodes [9,10,19,47]. LC activation in the epidermis and dermis consists of multiple events including CXCL10 production, morphological changes and down-regulation of cellular adhesion molecules, which are necessary for induction of adaptive immunity both in human and murine models [4,19,48]. In humans, TIV vaccination by the i.d. route induced systemic production of CXCL10, correlated with adaptive immune responses [15]. These inflammatory mediators also promote APCs activation as well as T cell activation and polarization [5–8].

In conclusion, to our knowledge, this study is the first to use an ex vivo human skin explant model for a multiparametric analysis, combining several approaches to determine modifications of metabolites, lipids, mRNA and proteins in response to cutaneous TIV administration. We explored early local cutaneous innate immune events, in the different skin layers, before any inflammatory reaction induced at the inoculation site. We found major modifications in protein profiles that differentiated vaccine-injected skin from control skin. These results add more insight into the molecular reaction in the skin that could be involved in changes in the behavior of cells following i.d. injection. Indeed, we previously showed that 4 h after MVA i.d. injection, LCs migrate to the dermis as shown by decrease in LC numbers, LC morphological changes (round shape LC) and CXCL10 production [18]. We also demonstrated these modifications are due to the release of IL-32 by keratinocyte which down regulates KC-LC adhesion [4]. In addition, in murine models, we showed that innate cell migration (neutrophils, inflammatory monocytes are detected in the skin between 4 and 8 h following i.d. injection of MVA or nanoparticles [10,19]. In our work protein networks are related to several cytokines/chemokines detected in the epidermis and dermis. These inflammatory molecules could be related to DCs/LCs activation status (such as CXCL10) which could orientate IFN $\gamma$ -type responses or participates to CD4 T cell activation

(such as CXCL10 and CCL22). This later chemokine is the ligand of CCR4 and help in positioning of T cell memory in the skin [49]. Neutrophils are attracted to the skin via CXCL8, however we observed a significant increase in CXCL10 mRNA at 18 h post-injection and not at early time points (< 4 h). This could be either due to dichotomy between either CXCL8 mRNA and protein secretion or the involvement of additional chemokines/chemokine receptors axis in early neutrophil trafficking [50]. We have also detected CX3CL1 mRNA suggesting initiation of monocyte trafficking to the skin. Finally, TNF- $\alpha$  could be involved in LC activation [51]. This study has demonstrated that proteomic analyses might enable the identification of potential early biomarkers of activated skin after vaccine administration by a cutaneous route.

## Declaration of Competing Interest

The authors have no financial conflicts of interest.

## Acknowledgment

The authors are grateful to the Dormeur Foundation, and Vaduz for providing the Cryostat HM550 apparatus, to Juliette Masure (Imabiotech) for technical help in MALDI-FTICR processing and to Jo-Ann Cahn for English editing. This project has received funding from the Agence National de Recherche (CE-16-0024-01). Behazine Combadière's laboratory has received funding from the Fondation pour la Recherche Médicale "Equipe FRM 2013" award.

## Appendix A. Supplementary data

Supplementary data to this article can be found online at <https://doi.org/10.1016/j.jprot.2020.103670>.

## References

- [1] B. Combadière, C. Liard, Transcutaneous and intradermal vaccination, *Hum. Vaccin.* 7 (2011) 811–827, <https://doi.org/10.4161/hv.7.8.16274>.
- [2] K. Kabashima, T. Honda, F. Ginhoux, G. Egawa, The immunological anatomy of the skin, *Nat. Rev. Immunol.* 19 (2019) 19, <https://doi.org/10.1038/s41577-018-0084-5>.
- [3] N. Romani, M. Thurnher, J. Idoyaga, R.M. Steinman, V. Flacher, Targeting of antigens to skin dendritic cells: possibilities to enhance vaccine efficacy, *Immunol. Cell Biol.* 88 (2010) 424–430, <https://doi.org/10.1038/icb.2010.39>.
- [4] J. Gonnert, H. Perrin, A.J. Hutton, D. Boccara, O. Bonduelle, M. Mimoun, et al., Interleukin-32 promotes detachment and activation of human Langerhans cells in a human skin explant model, *Br. J. Dermatol.* 179 (2018) 145–153, <https://doi.org/10.1111/bjd.16721>.
- [5] O. Berthier-Vergnes, F. Bermond, V. Flacher, C. Massacrier, D. Schmitt, J. Péguet-Navarro, TNF- $\alpha$  enhances phenotypic and functional maturation of human epidermal Langerhans cells and induces IL-12 p40 and IP-10/CXCL-10 production, *FEBS Lett.* 579 (2005) 3660–3668, <https://doi.org/10.1016/j.febslet.2005.04.087>.
- [6] M.D. Krathwohl, J.L. Anderson, Chemokine CXCL10 (IP-10) is sufficient to trigger an immune response to injected antigens in a mouse model, *Vaccine* 24 (2006) 2987–2993, <https://doi.org/10.1016/j.vaccine.2005.11.032>.
- [7] K. Ouwehand, S.J.A.M. Santegeerts, D.P. Bruynzeel, R.J. Scheper, Grujil T.D. de, S. Gibbs, CXCL12 is essential for migration of activated Langerhans cells from epidermis to dermis, *Eur. J. Immunol.* 38 (2008) 3050–3059, <https://doi.org/10.1002/eji.200838384>.
- [8] B. Nedoszytko, M. Sokółowska-Wojdyła, K. Ruckemann-Dziurdzińska, J. Roszkiewicz, R.J. Nowicki, Chemokines and cytokines network in the pathogenesis of the inflammatory skin diseases: atopic dermatitis, psoriasis and skin mastocytosis, *Postepy Dermatol. Alergol.* 31 (2014) 84–91, <https://doi.org/10.5114/pdia.2014.40920>.
- [9] V. Abadie, O. Bonduelle, D. Duffy, C. Parizot, B. Verrier, B. Combadière, Original encounter with antigen determines antigen-presenting cell imprinting of the quality of the immune response in mice, *PLoS One* 4 (2009) e8159, <https://doi.org/10.1371/journal.pone.0008159>.
- [10] D. Duffy, H. Perrin, V. Abadie, N. Benhabiles, A. Boissonnas, C. Liard, et al., Neutrophils transport antigen from the dermis to the bone marrow, initiating a source of memory CD8+ T cells, *Immunity* 37 (2012) 917–929, <https://doi.org/10.1016/j.immuni.2012.07.015>.
- [11] C. Buerger, N. Shirsath, V. Lang, A. Berard, S. Diehl, R. Kaufmann, et al., Inflammation dependent mTORC1 signaling interferes with the switch from keratinocyte proliferation to differentiation, *PLoS One* 12 (2017) e0180853, <https://doi.org/10.1371/journal.pone.0180853>.

- [12] S.W. Kashem, M. Haniffa, D.H. Kaplan, Antigen-presenting cells in the skin, *Annu. Rev. Immunol.* 35 (2017) 469–499, <https://doi.org/10.1146/annurev-immunol-051116-052215>.
- [13] R. Arakane, H. Nakatani, E. Fujisaki, A. Takahama, K. Ishida, M. Yoshiike, et al., Immunogenicity and safety of the new intradermal influenza vaccine in adults and elderly: a randomized phase 1/2 clinical trial, *Vaccine* 33 (2015) 6340–6350, <https://doi.org/10.1016/j.vaccine.2015.09.010>.
- [14] G.J. Gorse, A.R. Falsey, J.A. Fling, T.L. Poling, C.B. Strout, P.H. Tsang, Intradermally-administered influenza virus vaccine is safe and immunogenic in healthy adults 18–64 years of age, *Vaccine* 31 (2013) 2358–2365, <https://doi.org/10.1016/j.vaccine.2013.03.008>.
- [15] E. Gonçalves, O. Bonduelle, A. Soria, P. Loulergue, A. Rousseau, M. Cachanado, et al., Innate gene signature distinguishes humoral versus cytotoxic responses to influenza vaccination, *J. Clin. Invest.* 129 (2019) 1960–1971, <https://doi.org/10.1172/JCI125372>.
- [16] F. Marra, F. Young, K. Richardson, C.A. Marra, A meta-analysis of intradermal versus intramuscular influenza vaccines: immunogenicity and adverse events: meta-analysis of intradermal versus intramuscular influenza vaccines, *Influenza Other Respir. Viruses* 7 (2013) 584–603, <https://doi.org/10.1111/irv.12000>.
- [17] Y. Perez-Riverol, A. Csordas, et al., The PRIDE database and related tools and resources in 2019: improving support for quantification data, *Nucleic Acids Res* 47 (D1) (2019) D442–D450, <https://doi.org/10.1093/nar/gky1106>.
- [18] C. Liard, S. Munier, A. Joulin-Giet, O. Bonduelle, S. Hadam, D. Duffy, et al., Intradermal immunization triggers epidermal Langerhans cell mobilization required for CD8 T-cell immune responses, *J. Invest. Dermatol.* 132 (2012) 615–625, <https://doi.org/10.1038/jid.2011.346>.
- [19] C. Levin, O. Bonduelle, C. Nuttens, C. Primard, B. Verrier, A. Boissonnas, et al., Critical role for skin-derived migratory DCs and Langerhans cells in T FH and GC responses after intradermal immunization, *J. Invest. Dermatol.* 137 (2017) 1905–1913, <https://doi.org/10.1016/j.jid.2017.04.016>.
- [20] G. Li, Y.-Y. Li, J.-E. Sun, W. Lin, R. Zhou, ILK-PI3K/AKT pathway participates in cutaneous wound contraction by regulating fibroblast migration and differentiation to myofibroblast, *Lab. Invest.* 96 (2016) 741–751, <https://doi.org/10.1038/labinvest.2016.48>.
- [21] Y.-K. Lin, S.-H. Yang, C.-C. Chen, H.-C. Kao, J.-Y. Fang, Using Imiquimod-induced psoriasis-like skin as a model to measure the skin penetration of anti-psoriatic drugs, *PLoS One* 10 (2015), <https://doi.org/10.1371/journal.pone.0137890>.
- [22] W.A. Schroder, I. Anraku, T.T. Le, T.D.C. Hirata, H.I. Nakaya, L. Major, et al., SerpinB2 deficiency results in a stratum Corneum defect and increased sensitivity to topically applied inflammatory agents, *Am. J. Pathol.* 186 (2016) 1511–1523, <https://doi.org/10.1016/j.ajpath.2016.02.017>.
- [23] M.Q. Kwa, J. Huynh, J. Aw, L. Zhang, T. Nguyen, E.C. Reynolds, et al., Receptor-interacting protein kinase 4 and interferon regulatory factor 6 function as a signaling Axis to regulate keratinocyte differentiation, *J. Biol. Chem.* 289 (2014) 31077–31087, <https://doi.org/10.1074/jbc.M114.589382>.
- [24] A. Rebane, M. Zimmermann, A. Aab, H. Baurecht, A. Koreck, M. Karelson, et al., Mechanisms of IFN- $\gamma$ -induced apoptosis of human skin keratinocytes in patients with atopic dermatitis, *J. Allergy Clin. Immunol.* 129 (2012) 1297–1306, <https://doi.org/10.1016/j.jaci.2012.02.020>.
- [25] L.M. Wakim, N. Gupta, J.D. Mintern, J.A. Villadangos, Enhanced survival of lung tissue-resident memory CD8<sup>+</sup> T cells during infection with influenza virus due to selective expression of IFITM3, *Nat. Immunol.* 14 (2013) 238–245, <https://doi.org/10.1038/ni.2525>.
- [26] D. Rammath, K. Tunny, D.M. Hohenhaus, C.M. Pitts, A.-S. Bergot, P.M. Hogarth, et al., TLR3 drives IRF6-dependent IL-23p19 expression and p19/EBI3 heterodimer formation in keratinocytes, *Immunol. Cell Biol.* 93 (2015) 771–779, <https://doi.org/10.1038/icb.2015.77>.
- [27] G.C. Manara, G. Pasquinelli, L. Badiali-De Giorgi, C. Ferrari, S.A. Garatti, D. Fasano, et al., Human epidermal Langerhans cells express the ICAM-3 molecule. Immunohistochemical and immunoelectron microscopical demonstration, *Br. J. Dermatol.* 134 (1996) 22–27.
- [28] J. Neeffes, M.L.M. Jongsma, P. Paul, O. Bakke, Towards a systems understanding of MHC class I and MHC class II antigen presentation, *Nat. Rev. Immunol.* 11 (2011) 823–836, <https://doi.org/10.1038/nri3084>.
- [29] X. Ding, W. Bloch, S. Iden, M.A. Rüegg, M.N. Hall, M. Leptin, et al., mTORC1 and mTORC2 regulate skin morphogenesis and epidermal barrier formation, *Nat. Commun.* 7 (2016), <https://doi.org/10.1038/ncomms13226>.
- [30] T. Matsumura, T. Degawa, T. Takii, H. Hayashi, T. Okamoto, J. Inoue, et al., TRAF6-NF- $\kappa$ B pathway is essential for interleukin-1-induced TLR2 expression and its functional response to TLR2 ligand in murine hepatocytes, *Immunology* 109 (2003) 127–136, <https://doi.org/10.1046/j.1365-2567.2003.01627.x>.
- [31] D. Cretu, K. Liang, P. Saraon, I. Batruch, E.P. Diamandis, V. Chandran, Quantitative tandem mass-spectrometry of skin tissue reveals putative psoriatic arthritis biomarkers, *Clin. Proteomics* 12 (2015), <https://doi.org/10.1186/1559-0275-12-1>.
- [32] Y. Okada, B. Han, L.C. Tsoi, P.E. Stuart, E. Ellinghaus, T. Tejasvi, et al., Fine mapping major histocompatibility complex associations in psoriasis and its clinical subtypes, *Am. J. Hum. Genet.* 95 (2014) 162–172, <https://doi.org/10.1016/j.ajhg.2014.07.002>.
- [33] N. Qureshi, P.-Y. Perera, J. Shen, G. Zhang, A. Lenschat, G. Splitter, et al., The proteasome as a lipopolysaccharide-binding protein in macrophages: differential effects of proteasome inhibition on lipopolysaccharide-induced signaling events, *J. Immunol. Baltim. Md. 2003 (171) (1950)* 1515–1525, <https://doi.org/10.4049/jimmunol.171.3.1515>.
- [34] W. Bi, L. Zhu, Z. Zeng, X. Jing, Y. Liang, L. Guo, et al., Investigations into the role of 26S proteasome non-ATPase regulatory subunit 13 in neuroinflammation, *Neuroimmunomodulation* 21 (2014) 331–337, <https://doi.org/10.1159/000357811>.
- [35] D. Bonnel, R. Legouffe, A.H. Eriksson, R.W. Mortensen, F. Pamelard, J. Stauber, et al., MALDI imaging facilitates new topical drug development process by determining quantitative skin distribution profiles, *Anal. Bioanal. Chem.* 410 (2018) 2815–2828, <https://doi.org/10.1007/s00216-018-0964-3>.
- [36] I.S. Sørensen, C. Janfelt, M.M.B. Nielsen, R.W. Mortensen, N.Ø. Knudsen, A.H. Eriksson, et al., Combination of MALDI-MSI and cassette dosing for evaluation of drug distribution in human skin explant, *Anal. Bioanal. Chem.* 409 (2017) 4993–5005, <https://doi.org/10.1007/s00216-017-0443-2>.
- [37] Y. Sawada, T. Honda, S. Hanakawa, S. Nakamizo, T. Murata, Y. Ueharaguchi-Tanada, et al., Resolvin E1 inhibits dendritic cell migration in the skin and attenuates contact hypersensitivity responses, *J. Exp. Med.* 212 (2015) 1921–1930, <https://doi.org/10.1084/jem.20150381>.
- [38] H. Sigmundsdottir, J. Pan, G.F. Debes, C. Alt, A. Habtezion, D. Soler, et al., DCs metabolize sunlight-induced vitamin D3 to “program” T cell attraction to the epidermal chemokine CCL27, *Nat. Immunol.* 8 (2007) 285–293, <https://doi.org/10.1038/ni1433>.
- [39] N. Beyersdorf, N. Müller, Sphingomyelin breakdown in T cells: role in activation, effector functions and immunoregulation, *Biol. Chem.* 396 (2015) 749–758, <https://doi.org/10.1515/hsz-2014-0282>.
- [40] J.A. Carlsson, A.E. Wold, A.-S. Sandberg, S.M. Östman, The polyunsaturated fatty acids arachidonic acid and docosahexaenoic acid induce mouse dendritic cells maturation but reduce T-cell responses in vitro, *PLoS One* 10 (2015) e0143741, <https://doi.org/10.1371/journal.pone.0143741>.
- [41] A. Sala-Vila, E.A. Miles, P.C. Calder, Fatty acid composition abnormalities in atopic disease: evidence explored and role in the disease process examined, *Clin. Exp. Allergy J. Br. Soc. Allergy Clin. Immunol.* 38 (2008) 1432–1450, <https://doi.org/10.1111/j.1365-2222.2008.03072.x>.
- [42] H. Mellor, P.J. Parker, The extended protein kinase C superfamily, *Biochem. J.* 332 (Pt 2) (1998) 281–292.
- [43] A. Sharma, C.K. Maurya, D. Arha, A.K. Rai, S. Singh, S. Varshney, et al., Nod1-mediated lipolysis promotes diacylglycerol accumulation and successive inflammation via PKC $\delta$ -IRAK axis in adipocytes, *Biochim. Biophys. Acta Mol. Basis Dis.* 1865 (2019) 136–146, <https://doi.org/10.1016/j.bbdis.2018.10.036>.
- [44] C. Zeng, B. Wen, G. Hou, L. Lei, Z. Mei, X. Jia, et al., Lipidomics profiling reveals the role of glycerophospholipid metabolism in psoriasis, *GigaScience* 6 (2017), <https://doi.org/10.1093/gigascience/gix087>.
- [45] D. Ferrari, S. Gorini, G. Callegari, A. la Sala, Shaping immune responses through the activation of dendritic cells–P2 receptors, *Purinergic Signal* 3 (2007) 99–107, <https://doi.org/10.1007/s11302-006-9024-0>.
- [46] E. Lachmandas, A.B. Rios-Miguel, V.A.C.M. Koeken, E. van der Pasch, V. Kumar, V. Matzaraki, et al., Tissue metabolic changes drive cytokine responses to Mycobacterium tuberculosis, *J. Infect. Dis.* 218 (2018) 165–170, <https://doi.org/10.1093/infdis/jiy173>.
- [47] V. Abadie, Neutrophils rapidly migrate via lymphatics after Mycobacterium bovis BCG intradermal vaccination and shuttle live bacilli to the draining lymph nodes, *Blood* 106 (2005) 1843–1850, <https://doi.org/10.1182/blood-2005-03-1281>.
- [48] C. Liard, S. Munier, M. Arias, A. Joulin-Giet, O. Bonduelle, D. Duffy, et al., Targeting of HIV-p24 particle-based vaccine into differential skin layers induces distinct arms of the immune responses, *Vaccine* 29 (2011) 6379–6391, <https://doi.org/10.1016/j.vaccine.2011.04.080>.
- [49] C. Alanio, R.B. da Silva, D. Michonneau, P. Bouso, M.A. Ingersoll, M.L. Albert, CXCR3/CXCL10 axis shapes tissue distribution of memory phenotype CD8<sup>+</sup> T cells in nonimmunized mice, *J. Immunol.* 200 (2018) 139–146.
- [50] C.H. Kim, E.J. Kunkel, J. Boisvert, B. Johnston, J.J. Campbell, M.C. Genovese, et al., Bonzo/CXCR6 expression defines type 1-polarized T-cell subsets with extra-lymphoid tissue homing potential, *J. Clin. Invest.* 107 (2001) 595–601.
- [51] M. Cumberbatch, C.E. Griffiths, S.C. Tucker, R.J. Dearman, I. Kimber, Tumour necrosis factor- $\alpha$  induces Langerhans cell migration in humans, *Br. J. Dermatol.* 141 (1999) 192–200, <https://doi.org/10.1046/j.1365-2133.1999.02964.x>.